

Short communication

PtRh alloy nanoparticle electrocatalysts for oxygen reduction for use in direct methanol fuel cells

Kyung-Won Park^a, Dae-Seob Han^b, Yung-Eun Sung^{c,*}

^a Department of Chemical and Environmental Engineering, Soongsil University, Seoul 156-743, Republic of Korea

^b Battery Tech Center, LG Chemical Ltd., Research Park, Yu Song, Science Town, Taejon 305-380, Republic of Korea

^c School of Chemical and Biological Engineering & Research Center for Energy Conversion and Storage, Seoul National University, Seoul 151-744, Republic of Korea

Received 10 August 2005; received in revised form 20 March 2006; accepted 6 April 2006

Available online 5 June 2006

Abstract

PtRh alloy nanoparticles were synthesized for use in enhancing the stability of methanol crossover and electrocatalytic activity for oxygen reduction in direct methanol fuel cells (DMFCs). From the electrochemical results, by comparing Pt in terms of methanol tolerance and oxygen reduction with Pt-based alloys, the PtRh(2:1) was an optimum catalyst for the elimination of CO poisoning during the oxidation of crossover methanol as well as oxygen reduction. A PtRh(2:1) alloy cathode showed a higher power density as well as better performance stability than Pt in DMFC unit cell test.

© 2006 Elsevier B.V. All rights reserved.

Keywords: Direct methanol fuel cell; Cathode; Methanol tolerance; Nanoparticles; Platinum rhodium alloy

1. Introduction

Fuel cells using perfluorosulfonic ionomer membranes, such as Nafion membranes, have been the subject of considerable interest because they provide high power density at relatively low operating temperatures [1–3]. Two major difficulties that currently prevent commercial applications of DMFC are the low activity of anode and cathode catalysts at low temperatures [4,5] and loss of cell performance by methanol crossover through the polymer electrolyte membrane from the anode to the cathode. Methanol crossover lowers fuel utilization efficiency and results in poor cell performances, as the result of the poisoning of the Pt catalyst for oxygen reduction and a mixed potential by methanol oxidation at the cathode for oxygen reduction.

The mechanism of the electrochemical oxygen reduction reaction (ORR), as catalyzed by Pt has been extensively studied due to the importance of the design of cathodes for use in fuel cells [6,7]. A considerable loss in efficiency occurs in the cathode electrode, as the result of cathode overpotential [8,9]. The

overall reaction at the cathode of a fuel cell operating in an acid environment is shown below. Pt is typically used as a catalyst for oxygen electrode in acid media [10–13].



In fuel cells which use a perfluorosulfonic ionomer membrane, methanol crossover is a particularly important issue. Due to the permeation of methanol through the membrane, the cell voltage decreases significantly, causing a loss in performance and instability during long-term measurements accompanied by the poisoning of the Pt cathode catalyst and the creation of a mixed potential by methanol oxidation of the Pt catalyst. Thus, the development of an alternative to Pt as an oxygen reduction electrocatalyst has been an important issue for the last few decades. Typical materials which have methanol tolerant oxygen-reduction activity are elemental metals, such as Ru, Rh, Mo as well as their alloys. Recently Roy and co-workers investigated the oxygen reduction activity of carbon supported amorphous transition metal sulfides, MoRuS, RhRuS, RhMoS, ReRuS, etc., and in each case observed a high level of catalytic activity [14,15]. Schmidt et al. also investigated the ORR activity of both carbon supported Ru and a Ru-based chalcogenide and discovered marked difference between those and the

* Corresponding author. Tel.: +82 2 880 1889; fax: +82 2 888 1604.

E-mail address: ysung@snu.ac.kr (Y.-E. Sung).

standard ORR catalyst, Pt/Vulcan, namely that they are inactive with respect to methanol [16]. On the other hand, Watanabe and co-workers reported an enhanced oxygen reduction of Pt-based alloy electrodes, which are not actual nanoparticle systems, such as PtNi, PtCo, and PtFe in sulfuric acid [17,18].

In this paper, we report on the preparation of Rh-included cathode nanoparticle catalysts for the enhancement of stability for methanol crossover and oxygen reduction and an investigation of the structural properties and electrocatalytic activities of these catalysts. To confirm the stability of these catalysts to methanol crossover and methanol tolerance, galvanostatic endurance tests at constant current density were performed using a DMFC unit cell.

2. Experimental

Pt, PtRu and PtRh catalysts were prepared from $\text{H}_2\text{PtCl}_6 \cdot x\text{H}_2\text{O}$, $\text{RuCl}_3 \cdot x\text{H}_2\text{O}$ and $\text{RhCl}_3 \cdot x\text{H}_2\text{O}$ (Aldrich Chem. Co.) by synthesis method suggested previously [4,5]. The resulting particles were washed with deionized water and dried by freeze-drying in the absence of any heat treatment.

For structural analysis, TEM investigation was carried out using a Phillips CM20T/STEM Electron Microscope at an accelerating voltage of 200 kV and X-ray diffraction (XRD) patterns were obtained using a Rigaku X-ray diffractometer using $\text{Cu K}\alpha$ ($\lambda = 1.541 \text{ \AA}$) radiation. The diffraction peaks obtained were fitted by Lorentzian/Gaussian function to analyze the structural characteristics of the catalyst. X-ray photoelectron spectroscopy (XPS) was performed using a VG Scientific ESCALAB 200R X-ray photoelectron spectrometer. The X-ray source was Al $\text{K}\alpha$ operated at 1486.6 eV and 15 kV and 300 W. The XPS samples were prepared by coating the catalysts on the double side Cu tape (3M Inc.). The base pressure of the system was 5×10^{-10} Torr. The XPS core-level spectra were fitted to the Doniach–Sunjic line shape convoluted by a Gaussian contribution taking into account the spectrometer resolution.

Electrochemical measurements were investigated using a three-electrode cell at room temperature. Pt gauze and Ag/AgCl (in saturated KCl) were used as a counter and reference electrode, respectively. The working electrode was brushed with the catalyst ink consisting of 93 wt.% of metal catalyst and 7 wt.% of Nafion (Aldrich Co.) [4]. The metal loading (0.5 mg) of all tested samples was the same on the carbon electrode with 6 mm in diameter. Voltammetric curves in H_2SO_4 of 0.5 mol L^{-1} or CH_3OH $2 \text{ mol L}^{-1} + \text{H}_2\text{SO}_4$ 0.5 mol L^{-1} were recorded with an AUTOLAB of Eco Chemie (Netherlands) using rotating disk electrode system (628-10. Metrohm). The oxygen reduction current–potential curve was obtained from linear sweep scan voltammograms at various rotation frequencies in range of from 500 to 3000 rpm in an O_2 saturated $0.5 \text{ M H}_2\text{SO}_4$ solution. To observe the oxygen reduction current–potential in the existence of methanol, O_2 saturated solution was used at various rotation frequencies.

For a membrane–electrode-assembly (MEA) of DMFC, the anode of 5 mg cm^{-2} of PtRu (Johnson–Matthey Co.) and cathode of 5 mg cm^{-2} catalyst of Pt or PtRu or PtRh were formed on teflonized carbon paper (TGPH-090) substrates using cata-

lyst inks containing the appropriate weight percent of Nafion[®] ionomer solution (Aldrich Co.) [19]. The MEA for unit cell tests were fabricated by pressing as prepared cathode and anode layers onto both sides of a pre-treated Nafion[®] 117 electrolyte membrane at 110°C and 800 psi for 3 min. Cell performance was evaluated in a DMFC unit cell with a 2 cm^2 cross-sectional area, and measured with potentiometer (WMPG-3000), which recorded the cell under a constant current. Both fuel and oxidant flow paths were machined into graphite block end plates, which also served as current collectors. A 2 M methanol solution with a flow rate of $1 \text{ cm}^3 \text{ min}^{-1}$ was supplied by a Masterflex liquid micro-pump and dry O_2 flow was regulated at $500 \text{ cm}^3 \text{ min}^{-1}$ using a flow meter.

Cell performances were evaluated in a single cell within a 2 cm^2 cross-sectional area, and measured as the programmable electronic load. The fuel and oxidant flow paths were machined into graphite block end plates, which also served as current collectors. The cell temperature was maintained using heating lines embedded into each cell housing. A 2 M methanol solution, at $1 \text{ cm}^3 \text{ min}^{-1}$, was supplied by a Masterflex liquid micro-pump and dry O_2 was flowed without back pressure at $500 \text{ cm}^3 \text{ min}^{-1}$ by means of a flow meter.

3. Results and discussion

In general, it is well known that Pt is the best material for the cathode catalyst from the point of view of oxygen reduction. However, it is well known that the Pt surface is poisoned by CO or COH which are by-products of methanol oxidation. This poisoning effect ultimately results in instability as well as a reduction in cell performance. Thus, an alternate approach to prevent the loss of unit cell performance by methanol crossover and to assure the long-term stability of cell performance is to prevent the poisoning of Pt by removing the CO or COH on the Pt. According to bifunctional and electronic effects well-known in designing of alloy catalysts for methanol oxidation at anode in DMFC [1–4,20], Pt-based alloy catalysts can be prepared for oxygen reduction so that the Pt is not poisoned. During alloy formation the presence of a second metal should be able to remove CO poisoning of Pt catalysts and, at the same time, not affect the catalytic activity for oxygen reduction to any extent. In general, the PtRu alloy catalyst is well known as the best catalyst for methanol oxidation [21]. As seen above, since Rh has catalytic activity for oxygen reduction, PtRh cathode catalysts were also prepared by borohydride reduction. The 2θ of the (1 1 1) peak for PtRh(1:1), PtRh(2:1), and PtRh(3:1), which have angle shifts higher than the value of 39.83 for pure Pt, are 40.44 , 40.31 and 40.20 , respectively as seen in Fig. 1. The same trend was also shown in 2θ of the (2 0 0) and (2 2 0) peaks. The shifted angle was decreased according to the increase of Pt molar ratio. The higher angle shifts of the Pt peaks are consistent with alloy formation in the synthesized PtRh(x:1) between Pt and Rh. In addition, based on Debye–Scherrer equation, the average particle size of PtRh(x:1) catalysts is about 4–5 nm.

Fig. 2(a) shows TEM image of PtRh catalyst for oxygen reduction. The catalyst consists of nanoparticles of 4–5 nm, which is in good agreement with that obtained by XRD analysis.

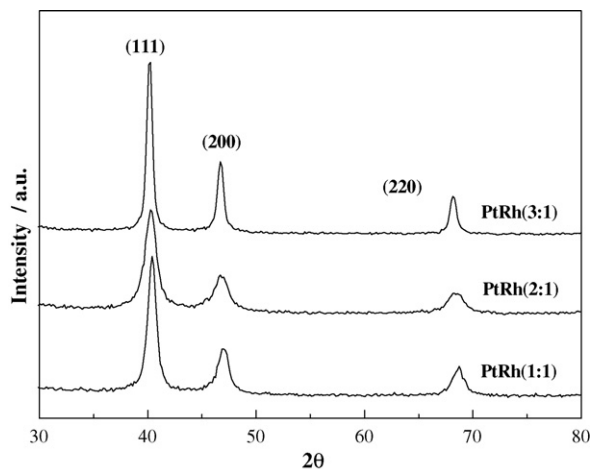


Fig. 1. X-ray diffraction patterns of PtRh alloy catalysts.

In addition, the nanostructured catalyst appeared to be relatively well dispersed. As shown in high resolution TEM image of Fig. 2(b), the lattice distance of PtRh nanoparticle is 0.226 nm which is larger than 0.228 nm of pure Pt(1 1 1). This means that Pt-based alloy catalyst by addition of smaller Rh atoms.

The electrocatalytic activity of the Pt and PtRh(*x*:1) alloy nanoparticles for methanol oxidation was investigated and the findings are shown in Fig. 3. PtRu nanoparticle showed the optimal catalytic activity for methanol oxidation. However, compared to the electrocatalytic activity of pure Pt and PtRh(*x*:1) alloy nanoparticles for methanol oxidation, the PtRh(2:1) alloy catalyst was also superior to Pt, showing a higher oxidation current and lower onset potential than pure Pt. Even if further studies are needed to clarify the mechanism of the enhanced activity of PtRh alloy, we conclude that the alloy may contribute to enhanced CO oxidation. One clue to this is the XPS study as shown in Fig. 4 [4]. In Fig. 4(a), Pt $4f_{7/2}$ and $4f_{5/2}$ lines appear at ~ 71 and ~ 74 eV, respectively, with the theoretical ratio of peak areas of 4–3. A comparison of the binding energies indicates that Pt is present in the zero-valence metallic state. On the other hand, peaks for Pt $^{2+}$ and Pt $^{4+}$ at 73.8 and 74.6 eV, respectively, were not present. It is noteworthy that the Pt-based nanoparticles contain only metallic a Pt phase, which provide sites for methanol (or oxygen) adsorption. It is obvious that the metallic Pt state is a requirement for excellent oxygen reduction current at the cathode as well as a high methanol oxidation current at the anode. Thus, in addition to this advantageous Pt state, the specific roles of the second metals and oxides in Pt-based nanoparticles lead to a higher activity than pure Pt. In Fig. 4(b), metallic rhodium appears as a spin-orbit doublet at 306.7 eV (Rh $3d_{5/2}$) and 311.4 eV (Rh $3d_{3/2}$). Rh $_2$ O $_3$ was characterized using the $3d_{5/2}$ and $3d_{3/2}$ peaks, present at 307.9 eV and 312.7 eV, respectively. As a result, it is likely that such a mixture of metallic and oxidative state leads to an enhancement in CO oxidation, the surface states of which play a role as an oxygen source for methanol oxidation.

The catalytic activity of PtRh alloys for oxygen reduction in an O $_2$ saturated H $_2$ SO $_4$ solution is shown in Fig. 5. In acidic media, pure Pt catalyst had the best performance for the oxy-

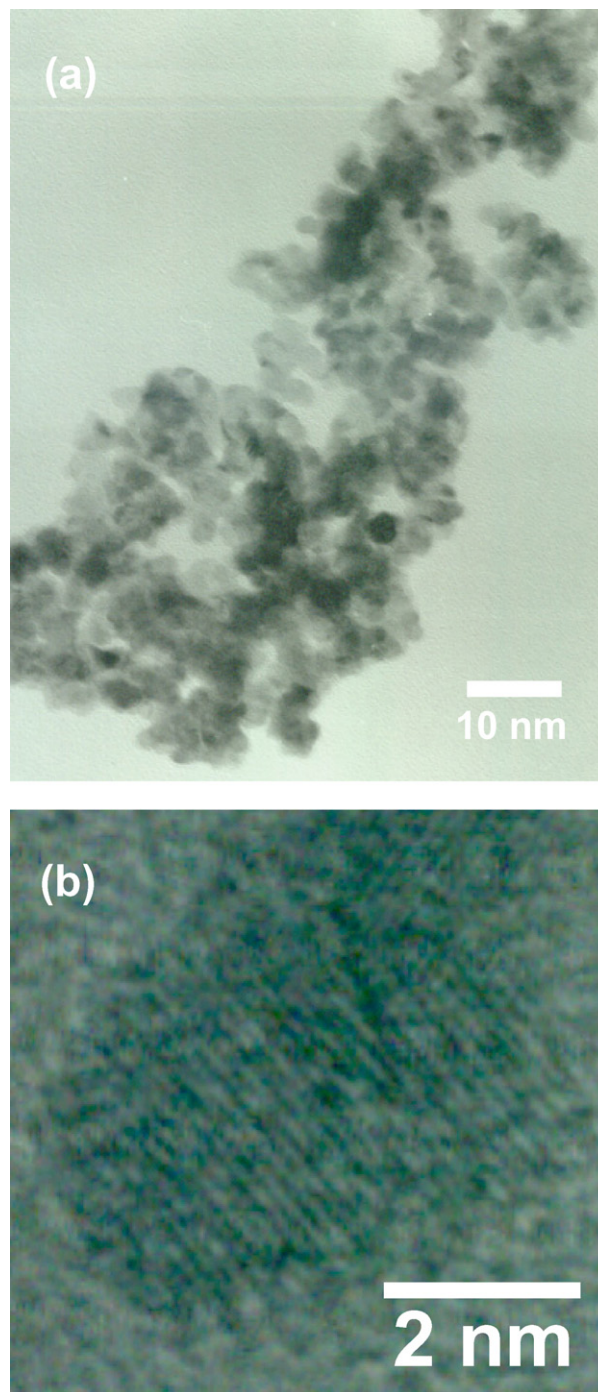


Fig. 2. (a) Transmission electron micrograph (TEM) image of PtRh nanosized electrocatalyst and (b) a high-resolution TEM (HRTEM) image having the lattice distance of PtRh alloy structure.

gen reduction reaction (ORR). On the other hand, PtRh(1:1) and PtRh(3:1) alloys were not functional as oxygen reduction catalysts. The activity of PtRu was also much lower than pure Pt in oxygen reduction. However, PtRh(2:1) showed considerable catalytic activity for oxygen reduction. From the electrochemical results shown in Figs. 3 and 5, PtRh(2:1) could be an optimum catalyst for the elimination of CO poisoning during the oxidation of crossover methanol as well as oxygen reduction.

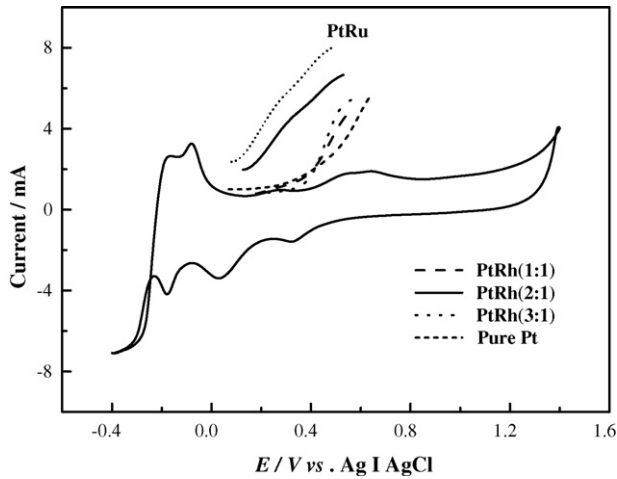


Fig. 3. Voltammetry of Pt, PtRu, and PtRh for methanol oxidation in 0.5 M $\text{H}_2\text{SO}_4 + 2 \text{ M CH}_3\text{OH}$. The solid base line represents a cyclic voltammetric curve for PtRh(2:1) in 0.5 M H_2SO_4 at 50 mV s^{-1} .

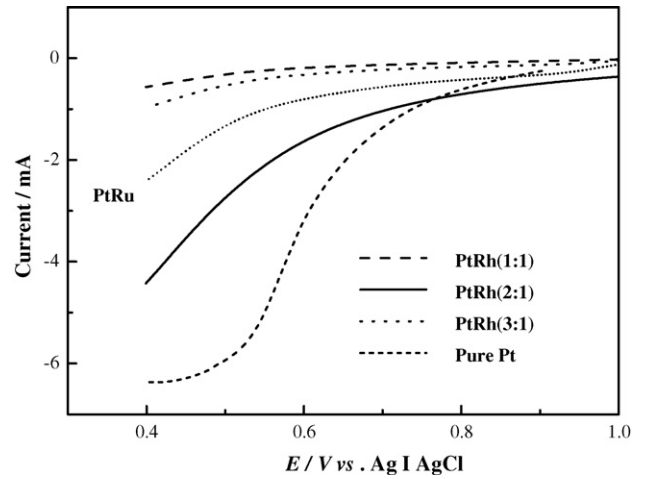
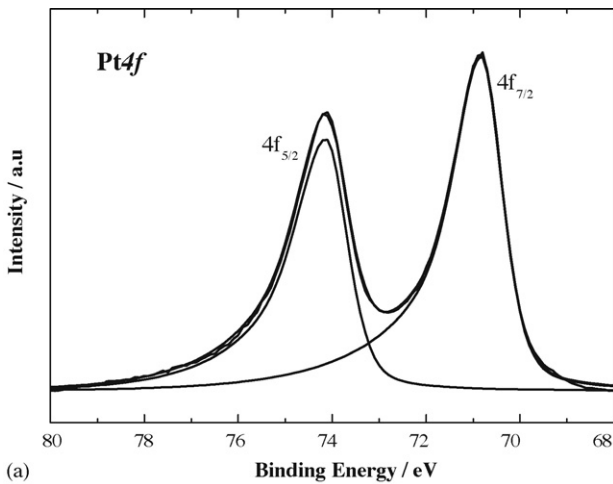
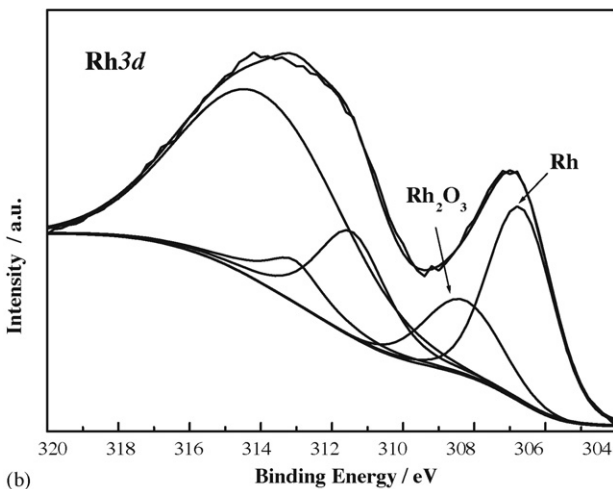


Fig. 5. Current–potential curves of Pt, PtRu, and PtRh for oxygen reduction in O_2 saturated 0.5 M H_2SO_4 at 50 mV s^{-1} .



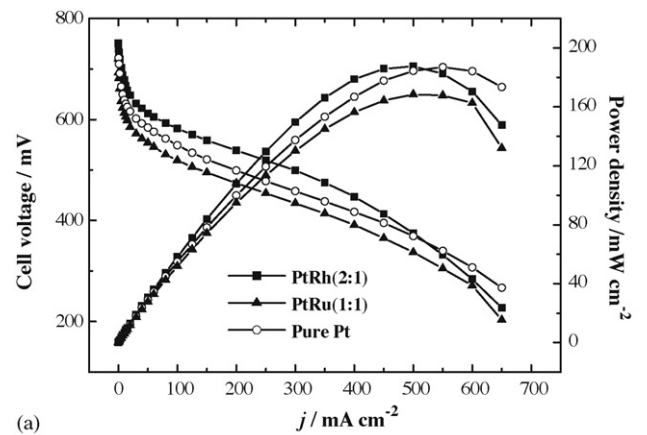
(a)



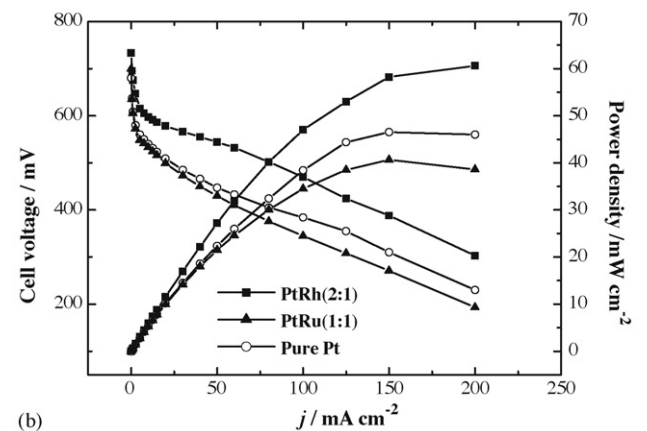
(b)

Fig. 4. X-ray photoelectron spectra of (a) Pt4f and (b) Rh3d in PtRh(2:1) catalysts.

Fig. 6 shows a comparison of DMFC performance according to cell temperature using PtRh(2:1), PtRu(1:1) and Pt as the cathode catalyst. In Fig. 5, the order of activity for oxygen reduction was pure Pt > PtRh(2:1) > PtRu(1:1). However, as shown in Fig. 6(a), the cell performances of pure Pt and PtRh(2:1) at 70°C are nearly the same but the case of the PtRu(1:1) cathode catalyst is the lowest. It is known that the performance of a DMFC at



(a)



(b)

Fig. 6. Comparison of DMFC performance using PtRh(2:1), PtRu(1:1) and Pt as the cathode catalyst at (a) 70°C and (b) 30°C .

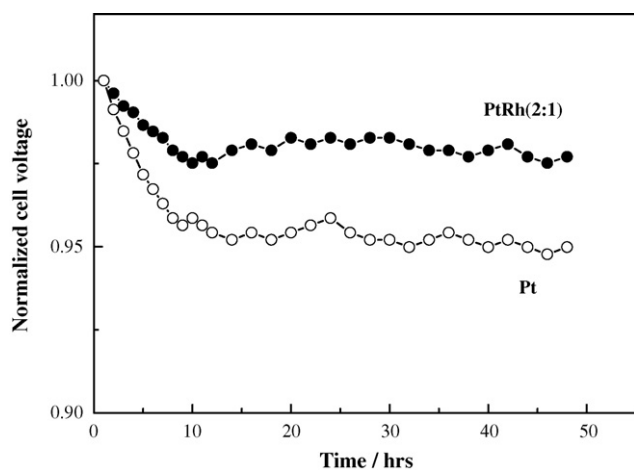


Fig. 7. Galvanostatic test of a DMFC at a constant current density using Pt and PtRh(2:1) as cathode catalyst. (PtRh(2:1) and Pt at 250 mA cm^{-2}).

low temperature, such as 30°C , is strongly affected by methanol crossover to the cathode through a Nafion membrane [5]. We found that the loss of power density by methanol crossover was 28, 18, and 14% at 30, 50, and 70°C , respectively, using a Nafion 117 membrane. This implies that the choice of cathode catalyst is very critical in a DMFC at low temperatures. As indicated in Fig. 6(b), cell performance for the case of PtRh(2:1) at 30°C is surprisingly superior to that for PtRu(1:1) and Pt as cathode catalysts. The open circuit voltages were 0.73, 0.70, and 0.69 V for PtRh(2:1), PtRu(1:1) and Pt, respectively. Cell performances were 60, 40 and 45 mW cm^{-2} at PtRh(2:1), PtRu(1:1) and Pt, respectively, an enhancement of more than 30%.

Fig. 7 shows data on galvanostatic test of a DMFC unit cell using different cathode catalysts measured at a constant current density. The normalization of voltage means measured voltage at any time divided by initial voltage at $t=0$. Compared with a pure Pt cathode, PtRh(2:1) maintained a high normalized cell voltage at the operation current density for 50 h. They continued with a 2–3% loss of initial voltage after 10 h. On the other hand, the cell voltage for pure Pt decreased rapidly to 5% of the initial value and, after 10 h, below 5%. This can be attributed to the mixed potential and CO poisoning of Pt by the oxidation of crossover methanol through the membrane. The PtRh(2:1) showed a high stability in a cell performance test. It is probable that this higher catalytic activity is the result of the removal of CO or COH from the Pt during crossover methanol oxidation by alloy formation with the Rh metal and thus increases the number of available sites for oxygen reduction. Consequently, we confirmed that PtRh(2:1) had a higher endurance than Pt and are promising as oxygen reduction catalysts in DMFC.

4. Conclusions

The oxygen reduction activity and methanol tolerance of PtRh nanoparticles were investigated for cathode catalyst in a DMFC system. Methanol crossover through a polymer elec-

trolyte membrane is known to result in a significant loss in performance in DMFC, especially at low temperatures. As a result, the methanol tolerance of oxygen reduction catalysts plays an important role in DMFC. The PtRh(2:1) had an enhanced activity for methanol oxidation and similar properties for oxygen reduction in acidic media compared with elemental Pt. From unit cell data, PtRh(2:1) was a superior oxygen reduction catalyst to pure Pt in DMFC, showing a more than 30% enhanced in performance at 30°C . It is concluded that the enhancement in unit cell performance and galvanostatic endurance were the result of the inhibition of CO poisoning on the Pt in the cathode.

Acknowledgments

This work (K. Park) was supported by the Soongsil University Research Fund. This work was supported by Korea Research Foundation (Grant #KRF-2004-005-00064) and KOSEF through the Research Center for Energy Conversion and Storage.

References

- [1] M.P. Hogarth, G.A. Hards, *Platinum Met. Rev.* 40 (1996) 150.
- [2] A. Hamnett, *Catal. Today* 38 (1997) 445.
- [3] A. Wieckowski, *Interfacial Electrochemistry*, Marcel-Decker, New York, 1999 (Chapters 44–51).
- [4] K.-W. Park, J.-H. Choi, B.-K. Kwon, S.-A. Lee, Y.-E. Sung, H.-Y. Ha, S.-A. Hong, H. Kim, A. Wieckowski, *J. Phys. Chem.* 106 (2002) 1869.
- [5] S.-A. Lee, K.-W. Park, J.-H. Choi, B.-K. Kwon, Y.-E. Sung, *J. Electrochem. Soc.* 106 (2002) 1869.
- [6] G. Tamizhmani, J.P. Dodelet, D. Guay, L. Dignard-Bailey, *J. Electroanal. Chem.* 444 (1998) 121.
- [7] E. Antolini, L. Giorgi, A. Pozio, E. Passalacqua, *J. Power Sources* 77 (1999) 136.
- [8] M. Sudoh, T. Kondoh, N. Kamiya, T. Ueda, K. Okajima, *J. Electrochem. Soc.* 147 (2000) 3739.
- [9] G. Fournier, G. Foubert, J.Y. Tiliquin, R. Core, D. Guay, J.P. Dodelet, *J. Electrochem. Soc.* 144 (1997) 145.
- [10] G. Tamizhmani, J.P. Dodelet, D. Guay, *J. Electrochem. Soc.* 143 (1996) 18.
- [11] Z. Sun, A.C.C. Tseung, *Electrochem. Solid-State Lett.* 3 (2000) 413.
- [12] U.A. Paulus, T.J. Schmidt, H.A. Gasteiger, R.J. Behm, *J. Electroanal. Chem.* 495 (2001) 134.
- [13] T.J. Schmidt, U.A. Paulus, H.A. Gasteiger, R.J. Behm, *J. Electroanal. Chem.* 508 (2001) 41.
- [14] R.W. Reeve, P.A. Christensen, A. Hamnett, S.A. Haydock, S.C. Roy, *J. Electrochem. Soc.* 145 (1998) 3463.
- [15] R.W. Reeve, P.A. Christensen, A.J. Dickinson, A. Hamnett, K. Scott, *Electrochim. Acta* 45 (2000) 4237.
- [16] T.J. Schmidt, U.A. Paulus, H.A. Gasteiger, N. Alonso-Vante, R.J. Behm, *J. Electrochem. Soc.* 147 (2000) 2620.
- [17] T. Toda, H. Igarashi, H. Uchida, M. Watanabe, *J. Electrochem. Soc.* 146 (1999) 3750.
- [18] T. Toda, H. Igarashi, M. Watanabe, *J. Electroanal. Chem.* 460 (1999) 258.
- [19] T. Hyeon, S. Han, Y.-E. Sung, K.-W. Park, Y.-W. Kim, *Angew. Chem. Int. Ed.* 42 (2003) 4352.
- [20] M. Watanabe, S. Motoo, *J. Electroanal. Chem.* 60 (1975) 275.
- [21] E. Herrero, K. Franaszczuk, A. Wieckowski, *J. Phys. Chem.* 98 (1994) 5074.